Published in final edited form as:
Bioconjug Chem. 2010 January ; 21(1): 111–121. doi:10.1021/bc900356g.

Controlled Synthesis of Camptothecin-Polylactide Conjugates and Nanoconjugates

Rong Tong and **Jianjun Cheng***
Department of Materials Science and Engineering, University of Illinois at Urban–Champaign, Urbana, Illinois 61821

Abstract

We report here a unique method of formulating camptothecin-polylactide (CPT-PLA) conjugate nanoparticles, termed nanoconjugates (NCs), through CPT/(BDI)ZnN(TMS)$_2$ [(BDI) = 2-((2,6-diisopropylphenyl)amido)-4-((2,6-bisalkyl)-imino)-2-pentene] mediated polymerization of lactide (LA) followed by nanoprecipitation. When CPT was used as the initiator to polymerize LA in the presence of (BDI)ZnN(TMS)$_2$, the polymerization was complete within hours with nearly 100% CPT loading efficiency and 100% LA conversion. CPT loading as high as 19.5% can be achieved for the CPT-polylactide (CPT-PLA) conjugate prepared at a LA/CPT ratio of 10. The steric bulk of the chelating ligands and the type of metals used had a dramatic effect on the initiation of the LA polymerization and the tendency of the ring opening of the CPT lactone. The CPT/(BDI)ZnN(TMS)$_2$-mediated LA polymerization yielded CPT-PLA conjugates with well controlled molecular weights and narrow molecular weight distributions (1.02–1.18). The nanoprecipitation of CPT-PLA led to the formation of NCs around 100 nm in size with narrow particle size distributions. Sustained release of CPT from CPT-PLA NCs was achieved without burst release. CPT-PLA NCs were toxic to PC-3 cells with tunable IC_{50} possible by adjusting the drug loading of the CPT-PLA NCs.

Keywords

Polymeric Nanoparticles; Drug Delivery; Cancer Therapy; Chemotherapeutics; Polymeric Nanomedicine; Conjugation; Camptothecin; Polymer-drug Conjugate; Polylactide

INTRODUCTION

20(S)-Camptothecin (CPT), a topoisomerase II inhibitor isolated from the Chinese tree *Camptotheca acuminate* in the 1960s, exhibits a broad range of anticancer activity in various animal models (1–2). CPT has low aqueous solubility in its therapeutically active lactone form. Once placed in an aqueous solution at physiological pH, the lactone form of CPT is quickly transformed to its carboxylate form, which is highly toxic and therapeutically inactive (3–5). Serum albumin preferentially binds to the carboxylate form of CPT and serves as the driving force of shifting the lactone-carboxylate equilibrium (shown in Scheme 1) toward the formation of the carboxylate (3–5). These pharmacological properties of CPT result in rapid deactivation and fast clearance of CPT from the circulation after it is intravenously administered. To overcome these drawbacks, CPT has been conjugated to various polymeric carriers for improved solubility, enhanced stability of its lactone form and reduced renal clearance (6–14).

*To whom correspondence should be addressed. jianjunc@illinois.edu. Tel: (217) 244-3924; Fax: (217) 333-2736; Address: Department of Materials Science and Engineering, University of Illinois at Urban–Champaign, Urbana, Illinois 61801.

Polymer-CPT conjugates prepared with conventional coupling chemistry have various heterogeneities that may impact their pharmacological and pharmacokinetic properties *in vivo*. For instance, various polymers used for the conjugation of CPT were prepared via condensation reaction with molecular weight distributions (MWDs) over a range of 1.5 to 2.5 (6,8). It is also difficult to control the site of CPT conjugation to polymers with pendant functional groups. Furthermore, the direct conjugation of CPT through its C20-hydroxyl groups is difficult multistep reaction; the CPT must first be converted to a CPT-amino ester and then conjugated to a polymer that contains carboxylate groups via the amine end group of the CPT-amino ester (12,15).

Here, we report a simple, unique chemistry that allows for one-step conjugation of CPT to the terminal carboxylate group of polylactide (PLA). Instead of using coupling chemistry, we developed a ring-opening polymerization method to facilitate the incorporation of CPT to PLA. Through a living polymerization, both the initiation (drug incorporation) and the chain propagation proceed in a well-controlled manner and result in materials with pre-defined drug loadings and MWDs in a range of 1.02–1.18. The resulting CPT-PLA conjugate was nanoprecipitated to form CPT-PLA conjugate nanoparticles, termed nanoconjugates (NCs), around 100 nm in size with narrow polydispersities and controlled antitumor toxicities.

EXPERIMENTAL PROCEDURES

General

$_{D,L}$-Lactide (LA) was purchased from TCI America (Portland, OR), recrystallized three times in toluene and stored at −30°C in a glove box prior to use. All of the anhydrous solvents were purified by alumina columns and kept anhydrous by using molecular sieves. CPT was purchased from LC Laboratories (Woburn, MA), dried and stored at −30°C in a glove box. Triethylamine (TEA) was dried with 4 Å molecular sieves overnight, transferred by a cannula under nitrogen to a dry flask that contained CaH_2, refluxed overnight, distilled and collected under nitrogen, and stored in a glove box over activated 4 Å molecular sieves. All other chemicals were purchased from Sigma-Aldrich (St Louis, MO) and used as received unless otherwise noted. The molecular weights (MWs) of PLA were determined by gel permeation chromatography (GPC also known as size exclusion chromatography (SEC)) equipped with an isocratic pump (Model 1100, Agilent Technology, Santa Clara, CA), a DAWN HELEOS 18-angle laser light scattering detector and an Optilab rEX refractive index detector (Wyatt Technology, Santa Barbara, CA). The wavelength of the HELEOS detector was set at 658 nm. The size exclusion columns (Phenogel columns 100 Å, 500 Å, 10^3 Å and 10^4 Å, 5 μm, 300 × 7.8 mm, Phenomenex, Torrance, CA) used for the analysis of polymers or polymer-drug conjugates were serially connected on the GPC. The GPC columns were eluted with THF (HPLC grade) at 40°C at 1 mL/min. HPLC analyses were performed on a System Gold system equipped with a 126P solvent module and a System Gold 128 UV detector (Beckman Coulter, Fullerton, CA). An analytical reverse phase (RP) column was utilized to separate CPT, CPT-succinic acid (CPT-SA) and other CPT derivatives. The NMR studies were conducted on a Varian UI500NB system (500 MHz). The sizes and the polydispersities of the PLA-CPT NCs were determined on a ZetaPALS dynamic light scattering (DLS) instrument (15 mW laser, incident beam = 676 nm, Brookhaven Instruments, Holtsville, NY). The lyophilization of the NCs was carried out on a benchtop lyophilizer (FreeZone 2.5, Fisher Scientific, PA). The BDI ligands (BDI-1 (16), BDI-2 (16), BDI-3 (16) and BDI-4 (17)) were synthesized by following the procedures previously reported. Synthesis and characterization of the corresponding metal complexes of these ligands were also previously reported (16–19). The low resolution electrospray ionization mass spectrometry (LR-ESI MS) experiments were performed on a Waters Quattro II mass spectrometer. The high resolution electrospray ionization mass spectrometry (HR-ESI MS) experiments were performed on a Micromass Q-TOF Ultima

system. The PC-3 cells (ATCC, Manassas, VA) used in the MTT (3-(4,5-dimethylthiazol-2-yl)-2,5-diphenyltetrazolium bromide) assay (20) were cultured in Ham's F12K medium containing 10% fetal bovine serum, 1000 units/mL aqueous penicillin G and 100 μg/mL streptomycin. The SEM analysis of NCs was conducted on a Hitachi-S4700 high resolution scanning electron microscope.

General Procedures for the Preparation of CPT-PLA Conjugate via CPT-Mediated Ring-Opening Polymerization of LA

(BDI-3)ZnN(TMS)$_2$ (5.5 mg, 8.9 μmol) was dissolved in anhydrous THF (300 μL). The solution was added to a vial containing CPT (3.0 mg, 8.6 mmol) and the mixture was stirred for 15 min until the CPT was completely dissolved in THF. LA (124 mg, 0.86 mmol) was dissolved in a vial containing THF (940 μL) and the resulting solution was added to the mixture of CPT/(BDI-3)ZnN(TMS)$_2$ ([LA]$_0$ = 0.69 M). FT-IR was used to follow the conversion of the LA in the polymerization solution by monitoring the intensity of the lactone band at 1772 cm^{-1}. After the LA was completely consumed, the polymerization was quenched with ice-cold methanol (10 mL). The precipitate (CPT-PLA) was collected by centrifugation and then dried under vacuum. The resulting CPT-PLA conjugate was denoted as CPT-LA$_n$ where *n* is the monomer/initiator (LA/CPT) molar ratio.

Reaction of CPT with Succinic Anhydride (SA) Mediated by Zn or Mg Catalysts

In a glove box, (BDI-3)ZnN(TMS)$_2$ (6.2 mg, 0.01 mmol) was dissolved in anhydrous THF (200 μL). The solution was added to a clean vial containing CPT (3.5 mg, 0.01 mmol) and THF (300 μL) and stirred for 15 min until the CPT was completely dissolved. SA (1.1 mg, 0.011 mmol) in THF (600 μL) was added and the vial was tightly sealed. It was then immediately taken out of the glove box and stirred for 4h at 40°C. The reaction was quenched with ice-cold methanol (1 mL). An aliquot of this solution was analyzed by HPLC equipped with an analytical C18 column (Luna C18(2), 250 × 4.6 mm, 5μ, Phenomenex, Torrance, CA). The mobile phase for the HPLC analysis was a solvent mixture containing equal volume of acetonitrile and water (0.1% TFA). All HPLC spectra were recorded and analyzed by a UV detector at 370 nm. The areas of the HPLC peaks of CPT and the CPT-SA were integrated and used for the quantification of their concentrations as compared to corresponding standard curves. An aliquot of the reaction mixture was also used for the MS analysis.

The CPT-SA used for NMR analysis was collected by preparative thin layer chromatography (prep-TLC, silica gel with a fluorescent indicator (254 nm), 1.5 mm thickness, Aldrich) and developed by ethyl acetate/methanol (v/v = 10/1). The R_f values of CPT and CPT-SA were 0.7 and 0.1, respectively. The silica gel was removed from the glass plate and the CPT-SA was extracted with methanol (2 × 30 mL). The methanol solution was then removed under vacuum; the resulting CPT-SA was analyzed by ^{1}H-NMR. ^{1}H-NMR (CD_3OD, 500 MHz): δ 8.63 (s, 1H, 7-H), 8.21 (d, J = 8.5 Hz, 1H, 12-H), 8.07 (d, J = 8.0 Hz, 1H, 9-H), 7.87 (td, J_t = 8.5 Hz, J_d = 1.5 Hz, 1H, 11-H), 7.71 (td, J_t = 8.0 Hz, J_d = 1.0 Hz, 1H, 10-H), 7.43 (s, 1H, 14-H), 5.57, 5.44 (AB, J_{AB} = 17.0 Hz, 2H, 17-H), 5.35 (s, 1H, 5-H), 2.81 (t, J = 7.5 Hz, 2H, -CH_2-COOH), 2.55 (t, J = 7.5 Hz, 2H, -CH_2-CH$_2$-COOH), 2.24 (m, 2H, 18-H), 0.99 (t, J = 8.0 Hz, 19-H). MS (LR-ESI, positive mode): calcualted for $C_{24}H_{20}N_2O_7$ $[M + H]^+$ m/z 449.1; found m/z 449.1. MS (HR-ESI, positive mode): calcualted for $C_{24}H_{20}N_2O_7$ $[M + H]^+$ m/z 449.1349; found m/z 449.1355.

General Procedure for the Formation and Characterization CPT-PLA Nanoconjugates (NCs)

A DMF solution containing the CPT-LA$_{10}$ conjugate (100 μL, 5 mg/mL) was added dropwise to nanopure water (4 mL). The resulting CPT-LA$_{10}$ NCs were collected by ultrafiltration (15 min, 3000 × *g*, Ultracel membrane with 10,000 NMWL, Millipore, Billerica, MA) and were

characterized by DLS and SEM for particle sizes and by HPLC for drug loading and release kinetics.

Hydrolysis of CPT-LA_{10} NCs

The CPT-LA_{10} NC in water (1 mL, 1 mg/mL) was treated with a NaOH solution (1M, 1 mL) for 12 h. The solution was then tuned to pH 2 by phosphoric acid addition, which resulted in a yellow solution. The solvent was removed by rotary evaporation. The resulting residue was then dissolved in acetonitrile/water (0.1% TFA) (v/v = 1/1) and injected into a semi-prep HPLC column (Jupitor Proteo 90 A, 250 × 21.20 mm, 10μ, Phenomenex, Torrance, CA). The fraction that had the identical elution time as the authentic CPT was collected. After the solvent was removed by vacuum, the resulting yellow oily residue was dissolved in phosphoric acid/methanol at a volume ratio of 1:1. The solution was tuned to pH 3–4 by 0.1 M NaOH and then extracted with chloroform (5 × 100 mL). The organic phase was combined and dried with $MgSO_4$. After the $MgSO_4$ was removed by filtration and the solvent was removed under vacuum, the resulting pale yellow solid was analyzed by ^{1}H-NMR. The ^{1}H-NMR spectrum of the CPT released from CPT-PLA NCs was identical to that of the authentic CPT (see Figure 6B) (21).

Release Kinetics of the CPT-LA_n NCs and the CPT/PLA Nanoparticle (NP)

CPT/PLA NPs were prepared through nanoprecipitation of CPT and PLA (MW = 1.5×10^4 g/mol) by following the procedures reported in literature (22). The CPT-LA_{10} NCs were prepared with CPT-LA_{10} conjugate by following the standard nanoprecipitation procedure described above. The NCs (or NPs) were collected and washed three times with nanopure water by ultrafiltration (Ultracel membrane 10,000 NMWL, Millipore, Billerica, MA). The NCs (or NPs) collected from the ultrafiltration device were dispersed in 1× PBS solution (pH = 7.4) (1 mg/mL) and incubated at 37°C. At selected time intervals, an aliquot of NCs (or NPs) (≈ 1 mL) was taken out of the incubator and centrifuged at 10,000 rpm for 10 min. The supernatant (500 μL) was carefully transferred to an Eppendorf tube using micropipette without disturbing the precipitates (NCs or NPs). The solution was tuned to pH 2 by phosphoric acid (85%) and the resulting solution was directly injected into HPLC equipped with an analytical pentafluorophenyl RP-column (Curosil-PFP, 250 × 4.6 mm, 5μ, Phenomenex, Torrance, CA). A mixture of acetonitrile and water (containing 0.1% TFA) at a volume ratio of 1:1 was used as the mobile phase. The flow rate was set at 1 mL/min. The area of the HPLC peak of the released CPT was intergraded for the quantification of CPT as compared to the standard curve for this drug.

Determination of the Cytotoxicity of CPT-LA_n NCs

PC-3 cells were placed in a 96-well plate for 24 h (10,000 cells per well). Cells were washed with 100 μL of pre-warmed PBS. Freshly prepared CPT-LA_{10}, CPT-LA_{25} and CPT-LA_{50} NCs (prepared in 1× PBS, 100 μL) were added to the cells. CPT was used as a positive control. Untreated cells were used as a negative control. PLA NPs without CPT being conjugated or encapsulated were prepared via the nanoprecipitation of the PLA with a MW of 14 kDa (22–23) and were subsequently used as a negative control in the MTT study. The PLA-NPs were applied to PC-3 cells at a concentration up to 0.5 μg/mL. The cells were incubated for 72 h in a 5% CO_2 incubator at 37°C. The standard MTT assay protocols were followed thereafter (20).

RESULTS AND DISCUSSION

(BDI)MN(TMS)$_2$/CPT (M=Zn, Mg)-Mediated Polymerization of Lactide

By mixing a hydroxyl-containing compound (ROH) with a metal-amido complex, M-OR, a highly active metal alkoxide, can be generated *in situ* that can be subsequently used to initiate a controlled polymerization of LA (24–26). Many well-designed M-ORs can quantitatively incorporate OR to the PLA termini with 100% monomer conversions (18–19,27–31). Recently, we demonstrated that hydroxyl-containing therapeutic agents with complex structures, such as paclitaxel and doxorubicin, can form coordination complexes with metal catalysts and subsequently initiate controlled LA polymerizations with the drug molecules being covalently attached to the PLA through ester linkers (32–33). Both paclitaxel and doxorubicin have complex molecular structures that contain multiple hydroxyl groups. By using rationally designed metal catalysts, we were able to control the polymerization to be initiated at one of the specific hydroxyl groups of these complex therapeutic molecules (32–33). In the context of expanding this drug-initiated ring-opening polymerization technique to other therapeutic molecules, we studied CPT-initiated LA polymerization.

We first tested the feasibility of forming CPT-metal complex. (BDI-1)MgN(TMS)$_2$ (Figure 1), a catalyst that we previously used in paclitaxel- and doxorubicin-mediated ROP of LA (32–33), was dissolved in THF. A colorless solution was obtained. We then added this solution to a vial containing CPT powder (1 equivalent relative to (BDI-1)MgN(TMS)$_2$). After the mixture was stirred for 20 min, it was noted that CPT was completely dissolved and the solution color gradually became orange. In the absence of (BDI-1)MgN(TMS)$_2$, however, CPT remained insoluble in THF and the solution stayed colorless. The sharp contrast of the solubility of CPT in the presence versus in the absence of (BDI-1)MgN(TMS)$_2$ as well as the color change after CPT was mixed with (BDI-1)MgN(TMS)$_2$ suggest possibly a coordination reaction between CPT and the (BDI-1)MgN(TMS)$_2$. (BDI-1)Mg-CPT alkoxide through the C20-OH of CPT is presumably the complex formed *in situ* via the coordination of (BDI-1)MgN (TMS)$_2$ and CPT (Figure 1).

We next examined if the mixture of (BDI-1)MgN(TMS)$_2$/CPT could initiate LA polymerization. After LA (100 equiv.) in THF was added dropwise to the (BDI-1)MgN (TMS)$_2$/CPT mixture, the polymerization proceeded rapidly and completed within 10 h with 100% LA conversion; the monomer conversion was followed by monitoring the intensity of the lactone band of LA at 1772 cm^{-1} on a FT-IR. One interesting observation was that the orange color of the polymerization solution gradually faded away during the course of polymerization, which indicated the segregation of the (BDI-1)Mg from CPT. This observation was in good agreement with the proposed reaction mechanism as shown in Figure 1a. After 100% LA conversion was achieved, the polymerization solution was analyzed by HPLC, which showed that CPT was completely incorporated to PLA with no detectable free CPT in the polymerization solution (data not shown). This observation was similar to what we observed in paclitaxel- and doxorubicin-initiated LA polymerization, both of which gave 100% drug incorporation efficiency in corresponding drug-initiated polymerization (32–33). The incorporation efficiency is also the initiation efficiency, which is the percent of therapeutic agent utilized in the initiation of LA polymerization and is equivalent to the encapsulation efficiency utilized in making NPs via non-covalent, encapsulation strategy. The M_n of the resulting CPT-PLA conjugate was 1.13×10^4 g/mol, which was in good agreement with the expected M_n (1.47×10^4 g/mol) (entry 1, Table 1). The molecular weight distribution (MWD) of the CPT-PLA conjugate, however, was relatively broad ($M_w/M_n = 1.31$) due in part to the chain transfer during polymerization (18). In our previous studies of paclitaxel and doxorubicin initiated LA polymerization, only the primary or the secondary hydroxyl groups of these drugs could efficiently initiate the polymerizations of LA (32–33). The present study demonstrated

for the first time that the C20-OH of CPT, a tertiary hydroxyl group, could also be activated by (BDI-1)MgN(TMS)$_2$ to initiate LA polymerization.

In order to achieve better controlled polymerization, we next tested (BDI-1)ZnN(TMS)$_2$, a Zn analogue of (BDI-1)MgN(TMS)$_2$. As reported by Coates and coworkers, Zn catalysts in general outperform Mg catalysts for LA polymerization (18). After (BDI-1)ZnN(TMS)$_2$ and CPT were mixed and stirred for 20 min, a light yellow solution was obtained. This (BDI-1)ZnN(TMS)$_2$/CPT complex mediated LA polymerization at an M/I ratio of 100 and gave CPT-PLA conjugate with a very narrow MWD (M_w/M_n = 1.07, entry 2, Table 1). However, the CPT incorporation efficiency was only 61% based on the HPLC analysis, indicating the poor efficiency of forming Zn-CPT complex during the initiation step. The actual M/I ratio in this reaction was 163 (calculated based on the LA/CPT ratio of 100:0.61). It was therefore not surprising that the obtained M_n (2.83×10^4 g/mol) was substantially higher than the M_n calculated based on the LA/CPT ratio of 100:1 (expected $M_n = 1.47 \times 10^4$ g/mol, entry 2, Table 1,). The poor efficiency for the coordination of CPT with (BDI-1)ZnN(TMS)$_2$ was due in part to the relatively low activity of Zn as compared to Mg as well as the steric bulk of BDI-1 ligand surrounding the coordination site (Figure 1b). We next studied whether enhanced incorporation efficiency of CPT could be achieved by using a Zn catalyst with a BDI ligand with reduced steric bulk and/or altered electronic property.

It has been reported that subtle change of BDI ligands can significantly affect the activity of (BDI)ZnN(TMS)$_2$ and its capability of controlling the polymerizations of cyclic esters or carbonates (16,34–38). Specifically, the 2, 6-substituents of the aryl groups (at the R^1 and R^2 positions) and the substitute at the R^3 position were found to have profound effects on the activities of the catalysts (Figure 1b) (17). We synthesized a series of zinc catalysts containing BDI ligands with variable 2, 6-aryl substituents and R^3 group (Figure 1b) and then used these catalysts in CPT-initiated LA polymerizations. We first checked the effect of the steric bulk of BDI on the LA polymerization. BDI-2 is an analogue of BDI-1 whose isopropyl (iPr) groups at both R^1 and R^2 position were replaced by ethyl (Et) groups; while BDI-3 is an analogue of BDI-1 whose iPr groups were replaced by Et groups only at both R^1 position. Both ligands were synthesized and used to prepare the corresponding (BDI)ZnN(TMS)$_2$ catalysts. As expected, the steric bulk of the BDI at its R^1 and R^2 positions had profound effect on the capability of the Zn catalysts to form coordination complexes with CPT during the initiation step. As compared to the 61% of incorporation efficiency observed with the use of (BDI-1)ZnN(TMS)$_2$, 100% incorporation efficiencies were observed in both (BDI-2)ZnN(TMS)$_2$/CPT and (BDI-3)ZnN(TMS)$_2$/CPT mediated polymerizations. The corresponding M_n's (2.01×10^4 g/mol and 1.73×10^4 g/mol, entries 3 and 4, Table 1) were much closer to the expected M_n than that of the PLA-CPT obtained from the (BDI-1)ZnN(TMS)$_2$/CPT mediated LA polymerization (entry 2, Table 1). Narrow MWDs ($M_w/M_n < 1.2$) were obtained for the CPT-PLA conjugates derived from (BDI-2)ZnN(TMS)$_2$/CPT and (BDI-3)ZnN(TMS)$_2$/CPT mediated polymerizations (entries 3 and 4, Table 1). BDI-4, an analogue of BDI-3 with a cyano group at the R^3 position (Figure 1b), was also prepared and studied. However, CPT remained insoluble in THF containing 1 equiv. (BDI-4)ZnN(TMS)$_2$, indicating the poor efficiency of forming (BDI-4)ZnN(TMS)$_2$/CPT coordination complex at room temperature. Thus, it was not surprising that the mixture of CPT and (BDI-4)ZnN(TMS)$_2$ could not initiate LA polymerization at room temperature (entry 5, Table 1). When this mixture of CPT and (BDI-4)ZnN(TMS)$_2$ was incubated at 40°C for 20–30 min, CPT was completely dissolved, suggesting the formation of (BDI-4)ZnN(TMS)$_2$/CPT coordination complex requires higher temperature. The CPT-PLA conjugate derived from (BDI-4)ZnN(TMS)$_2$/CPT-mediated LA polymerization had a high loading efficiency (98%) and a M_n very close to the expected molecular weight (entry 6, Table 1), but its MWD (M_w/M_n = 1.32, Table 1) was broader than the CPT-PLA conjugate derived from the (BDI-3)ZnN(TMS)$_2$/CPT-mediated polymerizations. Based on these preliminary studies, (BDI-3)ZnN(TMS)$_2$ was found to be the overall best catalyst with

respect to control over CPT incorporation and polymerization. (BDI-3)ZnN(TMS)$_2$ was therefore selected for further investigation for its capability of controlling polymerization of LA at various LA/CPT ratios.

Excellently controlled polymerizations were observed over a broad range of LA/CPT ratios from 75 to 400 when the LA polymerizations were mediated by (BDI-3)ZnN(TMS)$_2$/CPT (Table 2). Quantitative CPT incorporation efficiencies and very narrow MWDs (M_w/M_n = 1.02–1.18) were observed in all experiments performed. The obtained MWs of the CPT-PLA conjugates were in excellent agreement with the expected MWs (Table 2), which followed a linear correlation with the LA/CPT ratios (Figure 2a). Monomodal GPC MW distribution curves were observed in all CPT-PLA conjugates prepared with various LA/CPT ratios (Figure 2b). The well-controlled polymerization mediated by (BDI-3)ZnN(TMS)$_2$ likely proceeded through the conventional insertion-coordination mechanism (Scheme 2a).

Control of Initiation by (BDI)ZnN(TMS)$_2$ Catalysts

As mentioned earlier, the lactone ring of CPT should be preserved in order to maintain the antitumor activity of CPT. However, it is known that the lactone ring of CPT is unstable and subject to ring opening in the presence of a nucleophile. We next studied how the initiation could be specifically controlled at the C20-OH of CPT with negligible CPT lactone ring opening during (BDI)ZnN(TMS)$_2$/CPT initiated LA polymerizations.

In the initiation step, LA first reacts with (BDI)Zn-CPT alkoxide and then is inserted between the CPT and Zn to generate (BDI)Zn-lactide-CPT alkoxide, the new chain-propagating end group (Scheme 2a). CPT does not involve the subsequent chain propagation. Apparently, the most critical step determining whether the lactone ring of CPT is opened or remains closed is the initiation step. As LA is subject to rapid polymerization and the resulting CPT-PLA conjugate is difficult to be precisely characterized, we used succinic anhydride (SA) as the model monomer to study (BDI)ZnN(TMS)$_2$/CPT-mediated initiation. Such a reaction led to the formation of CPT-succinic acid (CPT-SA), a small molecule instead of a polymer, whose structure can be easily determined by routine characterization methods.

When just CPT and SA were mixed without addition of other reagents, no reaction occurred (entry 1, Table 3). Triethylamine (TEA), a non-nucleophilic base, has been used previously to facilitate the ring opening of SA by an alcohol (39). When TEA was added to the mixture of CPT and SA, the reaction was very slow and generated CPT-SA with a yield of 10.6% after the reaction mixture was incubated at 40°C for 12 h (peak z, Figure 3a-i; entry 2, Table 3). A substantial amount of CPT in its carboxylate form was also detected (peak x, Figure 3a-i), indicating that the lactone ring of CPT was unstable in the presence of TEA. In a control study, when naphthalene ethanol, an alcohol with a primary -OH group that is supposed be more reactive for nucleophilic reaction than the tertiary C20-OH of CPT, was used for the conjugation with SA in the presence of TEA, the yield of naphthalene-SA was 86.8% (data not shown).

N-(3-dimethylaminopropyl)-N’-ethylcarbodiimide (EDC), in conjunction with 4-(dimethylamino)-pyridine (DMAP), has been used previously for the conjugation of CPT with SA (40). When the reaction of CPT and SA was performed in the presence of EDC and DMAP at 40°C for 12 h, the yield of CPT-SA was only 12.8% (entry 3, Table 3), which was in good agreement with the previously reported result (40) and further confirmed the low activity of the tertiary C20-OH group of CPT.

We next studied the ring opening of SA by CPT in the presence of Mg or Zn catalysts. (BDI-1)MgN(TMS)$_2$-mediated conjugation of CPT and SA resulted in CPT-SA conjugates (Scheme 2b) with 59.5% yield when the reaction was carried out at 40°C for 4 h (entry 4, Table 3). CPT

in carboxylate form was also detected (peak x, Figure 3a-ii), indicating the CPT lactone ring was opened in the presence of (BDI-1)MgN(TMS)$_2$ and that it may function not only as a ROP catalyst but also as a strong base. The mechanism of ring opening remains elusive. When such a reaction was mediated by (BDI-1)ZnN(TMS)$_2$, a weaker base and a less reactive ROP catalyst compared to its Mg analogue, CPT-SA in 18.8% yield was obtained (entry 5, Table 3). Formation of small amount of CPT in its carboxylate form was also detected (peak x, Figure 3a-iii).

As shown in the polymerization study mentioned above (Table 1), the chelating BDI ligands have a significant impact on the activities of the BDI-metal complexes for LA polymerization. We tested (BDI-3)ZnN(TMS)$_2$, which was previously identified to be the best catalyst for CPT initiated LA polymerization, in this CPT/SA conjugation reaction. CPT-SA in 89.1% yield was obtained when the reaction of CPT and SA was carried out at 40°C for 4 h in the presence of (BDI-3)ZnN(TMS)$_2$ (entry 6, Table 3). The substantially increased yield of CPT-SA in this experiment indicated that (BDI-3)ZnN(TMS)$_2$ activated the tertiary C20-OH group of CPT very effectively to allow for facile nucleophilic ring opening of SA. Very interestingly, CPT-SA was the only product formed; no carboxylate form of CPT was detected (Figure 4a-iv). Excellently controlled ring opening of SA by CPT with no detectable CPT carboxylate was also observed with the use of (BDI-4)ZnN(TMS)$_2$ (Figure 3a-v), although the yield of the CPT-SA (71.7%, entry 7, Table 3) was not as high as that derived from the (BDI-3)ZnN(TMS)$_2$-mediated reaction(entry 6, Table 3).

The CPT-SA (peak z, Figure 3a-iv) was collected by preparative thin layer chromatography and analyzed by MS (Figure 3c) and ^{1}H NMR (Figure 3d–e). The high resolution MS analysis showed that the CPT-SA has a $[M + H]^+$ m/z= 449.1355, which was in excellent agreement with the expected $[M + H]^+$ m/z= 449.1349. To determine whether the SA ring was opened by the C17-OH (formed after the opening of the lactone ring of CPT) or by the C20-OH (Figure 3b), we compared the ^{1}H-NMR spectra of CPT-SA and CPT (Figure 3e). If the C17-OH mediated the ring opening of SA, the chemical shift of the C17-H of CPT-SA should change to some extent. However, as shown in Figure 3e, the chemical shift of the C17-H of CPT-SA was nearly identical to that of the authentic CPT (with a change of less than 0.03 ppm, Figure 3e), indicating that the lactone ring of CPT is well preserved in CPT-SA. In fact, the only major change of the chemical shifts among all the protons of CPT was the C18-H, which was shifted downfield from 1.97 ppm for CPT to 2.23 ppm for CPT-SA (Figure 3e). The only possible explanation is that the SA ring was opened by the C20-OH by CPT (Figure 3b). The high yield of CPT-SA obtained in this experiment indicated that (BDI-3)ZnN(TMS)$_2$ was capable of efficiently activating the C20-OH of CPT to facilitate the ring-opening reaction with SA. The CPT/SA ring-opening conjugation mediated by BDI-Zn catalyst appeared to be a versatile method for converting the C20-hydroxyl group of CPT to a carboxylic acid end group with a degradable ester linker, which can be further used for conjugation to various drug delivery vehicles through the conventional carboxylate-amine coupling chemistry.

Controlled Formation of CPT-PLA Nanoconjugates and Their in vitro Evaluation

CPT-PLA conjugated nanoparticles, termed nanoconjugates (NCs) in this study to differentiate them from the NPs prepared by co-precipitating drugs and polymers, were readily prepared through the nanoprecipitation of CPT-PLA conjugates (Figure 1a) after the metal and the BDI ligand were removed by solvent extraction. NCs less than 100 nm in size with narrow, monomodal particle distributions were readily obtained (Table 4 and Figure 4). The narrow size distributions and monomodal size distribution of NCs were in sharp contrast to the multimodal particle distributions frequently observed in the NPs prepared by the co-precipitation of polymers and drugs (22–23). It is not clear why NCs derived from the nanoprecipitation of PLA-CPT conjugates have such narrow size distributions (Figure 4a). As

the multimodal particle distributions in conventional NPs were attributed in part to the self-aggregation of the non-encapsulated drugs (22), the unimolecular structure of polymer-drug conjugates with reduced heterogeneities (low polymer polydispersities, controlled site of conjugation on CPT and PLA, absence of free CPT) may contribute to the formation of NCs with low particle polydispersity.

DLS can give quick assessment of the NP size and size distribution; however, the data should be treated with caution and compared with data collected by other techniques. When the same CPT-PLA NC was dried and analyzed by SEM (Figure 4b); the NC size distribution was found to be not as narrow as that observed in DLS (Figure 4a). As the particle sizes were assessed under different conditions using these two different techniques, it is unclear for the impact of the drying process for the SEM sample preparation on the particle size distribution. It should be noted, however, that both SEM and DLS analyses showed that there were no large aggregates (over 300–500 nm) as observed frequently in NPs prepared through the co-precipitation of polymers and drugs (22–23).

Because both monomer conversion and drug incorporation were quantitative (Table 4), the drug loadings of CPT-PLA NCs can be pre-determined by adjusting LA/CPT feeding ratios. At a low M/I ratio of 10, the drug loading of CPT-PLA NC can be as high as 19.5 % (CPT-LA_{10}, Table 4). To our knowledge, this CPT-PLA NC has by far one of the highest loadings of CPT ever reported (2,8).

We then studied the release kinetics of CPT from CPT-PLA NCs in PBS solution (pH = 7.4) at 37°C. Even at drug loading as high as 20%, sustained release of CPT from CPT-LA_{10} NC was observed through the hydrolysis of the ester linker that connects the CPT and the PLA (Figure 5a); roughly 40% of CPT was released from CPT-LA_{10} NC in 7 days with no burst release of CPT being observed (Figure 5a). This observation was in sharp contrast to the burst release of PLA/CPT NP that was prepared by the co-precipitation of CPT and PLA. In the latter system, the release of CPT depends entirely on diffusion of the drug from polymer matrices; as much as 97.1% of the encapsulated CPT was released from CPT/PLA NP when the NP was incubated in PBS for 24 h at 37°C (Figure 5a). The released CPT (in PBS, pH = 7.4, 37°C) has an HPLC elusion time identical to the authentic CPT (Figure 6a) and was confirmed to have the identical molecular structure as the authentic CPT after it was isolated and characterized by ^{1}H NMR (Figure 6b).

Cheng and co-workers have previously reported the synthesis and development of IT-101 (10–13), a CPT-cyclodextrin polymer conjugates with the drug molecule being conjugated to the polymeric carrier via a triglycinyl ester linker. IT-101 has been evaluated in numerous preclinical studies and a Phase-I human clinical study (41–43). Roughly 25% of the CPT in IT- 101 was released in 24 h when the release kinetics study was performed in PBS (pH = 7.4) at 37°C (12), whereas 15% of CPT was released from CPT-LA_{10} NC under similar condition (Figure 5). In CPT-LA_{10} NC, CPT is connected to PLA through a lactic ester bond, a linker with similar hydrophobicity and size as the glycinyl ester linker of IT-101. Because PLA is hydrophobic, the water and ions (H^+, OH^-) may not have as easy access to the lactic ester linker in CPT-PLA NC as to the glycinyl ester of IT-101 in which CPT is conjugated to hydrophilic cyclodextrin polymers. It is therefore not surprising to observe decreased CPT release rate in CPT-LA_{10} NC as compared to that of IT-101. It is anticipated that the release rate of CPT may further decrease when the pH value surrounding CPT-PLA NCs decreases from 7.4 to 5. This pH range is of particular importance and interest because it is well know that the cancerous tissues and the endosomes, where the NPs will be located following endocytosis, show pH changes in this range. The decreased hydrolysis rate of ester linkers may contribute to the antitumor efficacy *in vivo*. For instance, we found that trace amount of CPT in conjugated form in the harvested tumor tissues of mice could be detected by HPLC 109 days

after the administration of IT-101 (data not reported). Very surprisingly, the amount of CPT detected in tumor tissue was inversely proportional to the tumor size at Day 109. It is yet to be confirmed for the correlation of long-term tumor inhibition with the reduced release rates of CPT drug delivery system in slightly acidic environment.

The *in vitro* toxicities of CPT-PLA NCs were determined by MTT assays in PC-3 cells (Figure 5b). The IC_{50}'s of CPT-LA_{10}, CPT-LA_{25} and CPT-LA_{50} NCs with similar sizes (50–100 nm) were 389, 730, and 908 nM, respectively. The MTT studies revealed that the toxicity of the CPT-PLA NC, which was directly related to the release kinetics of CPT, could be tuned by the CPT loading in the NCs (Figure 5b). In general, NCs with higher drug loadings released drug more rapidly (32–33) and therefore showed higher toxicities (Figure 5b). This observation was presumably due to the fact that the NCs derived from the nanoprecipitation of the higher loading (lower MW) CPT-PLA conjugates have more loosely packed structures, as compared to the NCs derived from the lower loading (higher MW) CPT-PLA conjugates. Therefore, the ester linkers between CPT and PLA in the NCs with higher drug loadings were more accessible to the aqueous phase and were subject to faster hydrolysis. PLA NPs without CPT were used as a negative control and were found to show negligible toxicity to the PC-3 cells. The cell viability was 0.956 ± 0.003 when the PC-3 cells were incubated with the PLA NPs at a concentration of 0.5 μg/mL for 72 h at 37°C.

Conventional polymeric NPs prepared via co-precipitation of polymers and drugs have several formulation challenges that remain to be addressed (44–47). NPs typically exhibit a "burst" drug release in aqueous solution; as much as 80–90% of the encapsulated drugs are rapidly released during the first few to tens of hours (48). The rapid dose dumping may cause severe systemic toxicities (49). In addition, drug loadings in conventional NPs can be very low, typically in a range of 1–5% in most NPs studied (48,50–51). Drug loading of a delivery vehicle has been a critical measure of its utility in clinical settings (52–53). At lower drug loadings, a larger amount of delivery vehicles are needed. Due to the limited body weight and blood volume of animals, the administered volumes are usually fixed. For instance, the volume of a solution intravenously administered to mice with 20- to 30-g body weights should be controlled to below 100 μL (11). Intravenous administration of NPs with 1 wt% drug loading in a 100-μL solution at a dose of 50 mg/kg to a nude mouse with 20-g body weight requires the formulation of a concentrated, 1 g/mL NP solution, which is too viscous to formulate and inject intravenously. The third major challenge presented by NPs prepared via the encapsulation approach is the lack of a general strategy to achieve quantitative drug encapsulation. Depending on the amount of drug used, the hydrophobicity and hydrophilicity of the drug and the compatibility of the drug and polymer, the encapsulation efficiencies vary drastically over a range of 10 to 90% (48,54). Non-encapsulated drugs may self-aggregate (48) and can be very difficult to remove from the NPs. These formulation challenges significantly impact the processability and clinical translation of NP delivery vehicles prepared by drug/polymer co-precipitations.

PLA/CPT NPs prepared by the co-precipitation method have been previously reported to give low drug loading (0.1–1.5%), low loading efficiency (2.8–38.3%) and poorly controlled release kinetics (55). Depending on the formulation method, 20–90% of the encapsulated CPT was released within 1 h after the NP was exposed to the PBS solution. The ring-opening polymerization method that we developed allows for the incorporation of CPT to PLA with a tunable drug loading as high as 20 % and 100% loading efficiency (Table 4), which is in line with the high drug loading reported in polyglutamate-CPT conjugates (2,8). The unique conjugation technique allows for formation of CPT-containing PLA NCs with superbly controlled formulation parameters, which makes PLA-CPT NCs potentially useful agents for sustained treatment of cancer *in vivo*.

CONCLUSION

Preparation of PLA-drug conjugates with controlled drug loading and release profiles have been previously reported using conventional coupling chemistry (56–60). In this study we report a unique conjugation method that allows for CPT conjugation to PLA via CPT-initiated ROP of LA. This method allows for facile incorporation of CPT to PLA and forms PLA-CPT conjugates with low polydispersities, pre-determined drug loadings (as high as 20%) and 100% loading efficiencies. By controlling the metal and the chelating ligands of the catalysts, the initiation of LA polymerization can be specifically controlled at the C20-OH of CPT with negligible lactone ring opening in CPT. CPT conjugated to PLA should maintain its lactone form (the therapeutically active form). The BDI-metal chelating complexes do not have deleterious effects on CPT and can be easily removed by solvent extraction. Because both Zn and Mg ions are biocompatible (as key elements in our dietary mineral supplements), there should not be significant safety concerns regarding the use of these two metal catalysts for the ROP and formulation of NCs for potential clinical applications. Multi-gram scale of PLA-CPT conjugates can be readily prepared within hours using this one-pot polymerization approach. Because CPT molecules are covalently conjugated to PLA, the post-reaction formulation process (nanoprecipitation, purification, sterilization, lyophilization, shipping and handling, transporting, etc.) can be much more readily handled with a minimum change of sample property, in contrast to drug/polymer NPs prepared via encapsulation methods that struggle to prevent drug release during the formulation process. Given that the lack of a controlled formulation for nanoparticulate drug delivery vehicles presents bottlenecks to their clinical translation, this unique, ROP-mediated conjugation methodology may contribute to the development of clinically applicable, CPT and CPT-analogue based nanomedicines.

Acknowledgments

This work is supported by the National Science Foundation (Career Program DMR-0748834), the National Institute of Health (R21 grant 1R21CA139329-01), and the Siteman Center for Cancer Nanotechnology Excellence (SCCNE, Washington University)–the Center for Nanoscale Science and Technology (CNST, University of Illinois at Urban–Champaign). R.T. acknowledges a student fellowship from SCCNE. We would like to thank Professors Martin Burke and Jeffrey Moore for providing the anhydrous solvents.

LITERATURE CITED

1. Muggia FM, Dimery I, Arbuck SG. Camptothecin and its analogs. Ann. NY Acad. Sci 1996;803:213–223. [PubMed: 8993515]
2. Liehr, JG.; Giovanella, BC.; Verschraegen, CF. The Camptothecins: Unfolding Their Anticancer Potential (Annals of the New York Academy of Sciences). New York: New York Academy of Sciences; 2000.
3. Hertzberg RP, Caranfa MJ, Hecht SM. On the mechanism of topoisomerase-I inhibition by camptothecin-evidence for binding to an enzyme DNA complex. Biochemistry 1989;28:4629–4638. [PubMed: 2548584]
4. Mi Z, Burke TG. Differential interactions of camptothecin lactone and carboxylate forms with human blood components. Biochemistry 1994;33:10325–10336. [PubMed: 8068669]
5. Mi Z, Burke TG. Marked interspecies variations concerning the interactions of camptothecin with serum albumins: a frequency-domain fluorescence spectroscopic study. Biochemistry 1994;33:12540–12545. [PubMed: 7918477]
6. Greenwald RB, Pendri A, Conover C, Gilbert C, Yang R, Xia J. Drug delivery systems .2. Camptothecin 20-O-poly(ethylene glycol)ester transport forms. J. Med. Chem 1996;39:1938–1940. [PubMed: 8642549]
7. Dharap SS, Wang Y, Chandna P, Khandare JJ, Qiu B, Gunaseelan S, Sinko PJ, Stein S, Farmanfarmaian A, Minko T. Tumor-specific targeting of an anticancer drug delivery system by LHRH peptide. Proc. Natl. Acad. Sci. U. S. A 2005;102:12962–12967. [PubMed: 16123131]

8. Bhatt RL, de Vries P, Tulinsky J, Bellamy G, Baker B, Singer JW, Klein P. Synthesis and in vivo antitumor activity of poly(L-glutamic acid) conjugates of 20(S)-camptothecin. J. Med. Chem 2003;46:190–193. [PubMed: 12502373]
9. Cabral H, Nakanishi M, Kumagai M, Jang WD, Nishiyama N, Kataoka K. A Photo-Activated Targeting Chemotherapy Using Glutathione Sensitive Camptothecin-Loaded Polymeric Micelles. Pharm. Res 2009;26:82–92. [PubMed: 18758920]
10. Schluep T, Cheng J, Khin KT, Davis ME. Pharmacokinetics and biodistribution of the camptothecin-polymer conjugate IT-101 in rats and tumor-bearing mice. Cancer Chemothera. Pharmacol 2006;57:654–662.
11. Cheng J, Khin KT, Davis ME. Antitumor Activity of beta-Cyclodextrin Polymer-Camptothecin Conjugates. Mol. Pharm 2004;1:183–193. [PubMed: 15981921]
12. Cheng JJ, Khin KT, Jensen GS, Liu AJ, Davis ME. Synthesis of linear, beta-cyclodextrin-based polymers and their camptothecin conjugates. Bioconjugate Chem 2003;14:1007–1017.
13. Schluep T, Hwang J, Cheng J, Heidel JD, Bartlett DW, Hollister B, Davis ME. Preclinical efficacy of the camptothecin-polymer conjugate IT-101 in multiple cancer models. Clin. Cancer Res 2006;12:1606–1614. [PubMed: 16533788]
14. Schluep T, Hwang J, Hildebrandt IJ, Czernin J, Choi CHJ, Alabi CA, Mack BC, Davis ME. Pharmacokinetics and tumor dynamics of the nanoparticle IT-101 from PET imaging and tumor histological measurements. Proc. Natl. Acad. Sci. U. S. A 2009;106:11394–11399. [PubMed: 19564622]
15. Greenwald RB, Pendri A, Conover CD, Lee C, Choe YH, Gilbert C, Martinez A, Xia J, Wu DC, Hsue M. Camptothecin-20-PEG ester transport forms: the effect of spacer groups on antitumor activity. Bioorg. Med. Chem 1998;6:551–562. [PubMed: 9629468]
16. Moore DR, Cheng M, Lobkovsky EB, Coates GW. Mechanism of the alternating copolymerization of epoxides and CO2 using beta-diiminate zinc catalysts: Evidence for a bimetallic epoxide enchainment. J. Am. Chem. Soc 2003;125:11911–11924. [PubMed: 14505413]
17. Jeske RC, DiCiccio AM, Coates GW. Alternating copolymerization of Epoxides and cyclic anhydrides: An improved route to aliphatic polyesters. J. Am. Chem. Soc 2007;129:11330–11331. [PubMed: 17722928]
18. Chamberlain BM, Cheng M, Moore DR, Ovitt TM, Lobkovsky EB, Coates GW. Polymerization of lactide with zinc and magnesium beta-diiminate complexes: Stereocontrol and mechanism. J. Am. Chem. Soc 2001;123:3229–3238. [PubMed: 11457057]
19. Cheng M, Moore DR, Reczek JJ, Chamberlain BM, Lobkovsky EB, Coates GW. Single-site beta-diiminate zinc catalysts for the alternating copolymerization of CO2 and epoxides: Catalyst synthesis and unprecedented polymerization activity. J. Am. Chem. Soc 2001;123:8738–8749. [PubMed: 11535078]
20. Martin-Kleiner I, Svoboda-Beusan I, Gabrilovac J. PMA and doxorubicin decrease viability, MTT activity and expression of CD10 marker on NALM-1 leukemic cells. Immunopharma. Immunotox 2006;28:411–420.
21. Conover CD, Greenwald RB, Pendri A, Shum KL. Camptothecin delivery systems: the utility of amino acid spacers for the conjugation of camptothecin with polyethylene glycol to create prodrugs. Anti-Cancer Drug Design 1999;14:499–506. [PubMed: 10834271]
22. Cheng J, Teply BA, Sherifi I, Sung J, Luther G, Gu FX, Levy-Nissenbaum E, Radovic-Moreno AF, Langer R, Farokhzad OC. Formulation of functionalized PLGA-PEG nanoparticles for in vivo targeted drug delivery. Biomaterials 2007;28:869–876. [PubMed: 17055572]
23. Farokhzad OC, Cheng J, Teply BA, Sherifi I, Jon S, Kantoff PW, Richie JP, Langer R. Targeted nanoparticle-aptamer bioconjugates for cancer chemotherapy in vivo. Proc. Natl. Acad. Sci. U. S. A 2006;103:6315–6320. [PubMed: 16606824]
24. Dechy-Cabaret O, Martin-Vaca B, Bourissou D. Controlled ring-opening polymerization of lactide and glycolide. Chem. Rev 2004;104:6147–6176. [PubMed: 15584698]
25. Coulembier O, Degee P, Hedrick JL, Dubois P. From controlled ring-opening polymerization to biodegradable aliphatic polyester: Especially poly(beta-malic acid) derivatives. Prog. Polym. Sci 2006;31:723–747.
26. Okada M. Chemical syntheses of biodegradable polymers. Prog. Polym. Sci 2002;27:87–133.

27. Kuran W. Coordination polymerization of heterocyclic and heterounsaturated monomers. Prog. Polym. Sci 1998;23:919–992.
28. Chisholm MH, Eilerts NW. Single-site metal alkoxide catalysts for ring-opening polymerizations. Poly(dilactide) synthesis employing {HB(3-Bu(t)pz)(3)}Mg(OEt). Chem. Commun 1996:853–854.
29. O'Keefe BJ, Hillmyer MA, Tolman WB. Polymerization of lactide and related cyclic esters by discrete metal complexes. J. Chem. Soc., Dalton Trans 2001:2215–2224.
30. Williams CK, Breyfogle LE, Choi SK, Nam W, Young VG, Hillmyer MA, Tolman WB. A highly active zinc catalyst for the controlled polymerization of lactide. J. Am. Chem. Soc 2003;125:11350–11359. [PubMed: 16220958]
31. O'Keefe BJ, Monnier SM, Hillmyer MA, Tolman WB. Rapid and controlled polymerization of lactide by structurally characterized ferric alkoxides. J. Am. Chem. Soc 2001;123:339–340. [PubMed: 11456524]
32. Tong R, Cheng J. Paclitaxel-initiated, controlled polymerization of lactide for the formulation of polymeric nanoparticulate delivery vehicles. Angew. Chem., Int. Ed 2008;47:4830–4834.
33. Tong R, Cheng J. Ring-Opening Polymerization-Mediated Controlled Formulation of Polylactide-Drug Nanoparticles. J. Am. Chem. Soc 2009;131:4744–4754. [PubMed: 19281160]
34. Allen SD, Moore DR, Lobkovsky EB, Coates GW. High-activity, single-site catalysts for the alternating copolymerization of CO2 and propylene oxide. J. Am. Chem. Soc 2002;124:14284–14285. [PubMed: 12452684]
35. Coates GW, Moore DR. Discrete metal-based catalysts for the copolymerization CO2 and epoxides: Discovery, reactivity, optimization, and mechanism. Angew. Chem., Int. Ed 2004;43:6618–6639.
36. Rieth LR, Moore DR, Lobkovsky EB, Coates GW. Single-site beta-diiminate zinc catalysts for the ring-opening polymerization of beta-butyrolactone and beta-valerolactone to poly(3-hydroxyalkanoates). J. Am. Chem. Soc 2002;124:15239–15248. [PubMed: 12487599]
37. Rowley JM, Lobkovsky EB, Coates GW. Catalytic double carbonylation of epoxides to succinic anhydrides: Catalyst discovery, reaction scope, and mechanism. J. Am. Chem. Soc 2007;129:4948–4960. [PubMed: 17397149]
38. Moore DR, Cheng M, Lobkovsky EB, Coates GW. Electronic and steric effects on catalysts for CO2/epoxide polymerization: Subtle modifications resulting in superior activities. Angew. Chem., Int. Ed 2002;41:2599–2602.
39. Spivey AC, Andrews BI. Catalysis of the asymmetric desymmetrization of cyclic anhydrides by nucleophilic ring-opening with alcohols. Angew. Chem., Int. Ed 2001;40:3131–3134.
40. Lu H, Lin HX, Jiang Y, Zhou XG, Wu BL, Chen JM. Synthesis and antitumor activity of 20-O-linked succinate-based camptothecin ester derivatives. Lett. Drug Des. Discov 2006;3:83–86.
41. Yen Y, Synold T, Schluep T. First-in-human phase I trial of a cyclodextrincontaining polymer-camptothecin nanoparticle in patients with various solid tumors. J. Clin. Oncol 2007;25(Suppl 18):14078.
42. Heath JR, Davis ME. Nanotechnology and cancer. Annu. Rev. Med 2008;59:251–265. [PubMed: 17937588]
43. Davis ME, Chen Z, Shin DM. Nanoparticle therapeutics: an emerging treatment modality for cancer. Nat. Rev. Drug Discovery 2008;7:771–782.
44. Tong R, Cheng J. Anticancer polymeric nanomedicines. Polymer Reviews 2007;47:345–381.
45. Tong R, Christian DA, Tang L, Cabral H, Baker JR, Kataoka K, Discher DE, Cheng JJ. Nanopolymeric Therapeutics. MRS Bulletin 2009;34:422–431.
46. Teply BA, Tong R, Jeong SY, Luther G, Sherifi I, Yim CH, Khadernhosseini A, Farokhzad OC, Langer RS, Cheng J. The use of charge-coupled polymeric microparticles and micromagnets for modulating the bioavailability of orally delivered macromolecules. Biomaterials 2008;29:1216–1223. [PubMed: 18082254]
47. Cheng JJ, Teply BA, Jeong SY, Yim CH, Ho D, Sherifi I, Jon S, Farokhzad OC, Khademhosseini A, Langer RS. Magnetically responsive polymeric microparticles for oral delivery of protein drugs. Pharm. Res 2006;23:557–564. [PubMed: 16388405]
48. Musumeci T, Ventura CA, Giannone I, Ruozi B, Montenegro L, Pignatello R, Puglisi G. PLA/PLGA nanoparticles for sustained release of docetaxel. Int. J. Pharm 2006;325:172–179. [PubMed: 16887303]

49. Matsumura Y, Hamaguchi T, Ura T, Muro K, Yamada Y, Shimada Y, Shirao K, Okusaka T, Ueno H, Ikeda M, Watanabe N. Phase I clinical trial and pharmacokinetic evaluation of NK911, a micelle-encapsulated doxorubicin. Br. J. Cancer 2004;91:1775–1781. [PubMed: 15477860]
50. Mu L, Feng SS. A novel controlled release formulation for the anticancer drug paclitaxel (Taxol(R)): PLGA nanoparticles containing vitamin E TPGS. J. Controlled Release 2003;86:33–48.
51. Avgoustakis K. Pegylated Poly(Lactide) and Poly(Lactide-co-Glycolide) Nanoparticles: Preparation, Properties and Possible Application in drug Delivery. Curr. Drug Delivery 2004;1:321–333.
52. Hamblett KJ, Senter PD, Chace DF, Sun MMC, Lenox J, Cerveny CG, Kissler KM, Bernhardt SX, Kopcha AK, Zabinski RF, Meyer DL, Francisco JA. Effects of drug loading on the antitumor activity of a monoclonal antibody drug conjugate. Clin. Cancer Res 2004;10:7063–7070. [PubMed: 15501986]
53. Barenholz Y. Relevancy of drug loading to liposomal formulation therapeutic efficacy. J. Liposome Res 2003;13:1–8. [PubMed: 12725720]
54. Missirlis D, Kawamura R, Tirelli N, Hubbell JA. Doxorubicin encapsulation and diffusional release from stable, polymeric, hydrogel nanoparticles. Eur. J. Pharm. Sci 2006;29:120–129. [PubMed: 16904301]
55. Kunii R, Onishi H, Machida Y. Preparation and antitumor characteristics of PLA/(PEG-PPG-PEG) nanoparticles loaded with camptothecin. Eur. J. Pharm. Biopharm 2007;67:9–17. [PubMed: 17337172]
56. Lee CC, Gillies ER, Fox ME, Guillaudeu SJ, Frechet JMJ, Dy EE, Szoka FC. A single dose of doxorubicin-functionalized bow-tie dendrimer cures mice bearing C-26 colon carcinomas. Proc. Natl. Acad. Sci. U. S. A 2006;103:16649–16654. [PubMed: 17075050]
57. Yoo HS, Lee KH, Oh JE, Park TG. In vitro and in vivo anti-tumor activities of nanoparticles based on doxorubicin-PLGA conjugates. J. Controlled Release 2000;68:419–431.
58. Yokoyama M, Miyauchi M, Yamada N, Okano T, Sakurai Y, Kataoka K, Inoue S. Polymer Micelles as Novel Drug Carrier - Adriamycin-Conjugated Poly(Ethylene Glycol) Poly(Aspartic Acid) Block Copolymer. J. Controlled Release 1990;11:269–278.
59. Sengupta S, Eavarone D, Capila I, Zhao GL, Watson N, Kiziltepe T, Sasisekharan R. Temporal targeting of tumour cells and neovasculature with a nanoscale delivery system. Nature 2005;436:568–572. [PubMed: 16049491]
60. Zhang ZP, Feng SS. Nanoparticles of poly(lactide)/vitamin E TPGS copolymer for cancer chemotherapy: Synthesis, formulation, characterization and in vitro drug release. Biomaterials 2006;27:262–270. [PubMed: 16024075]

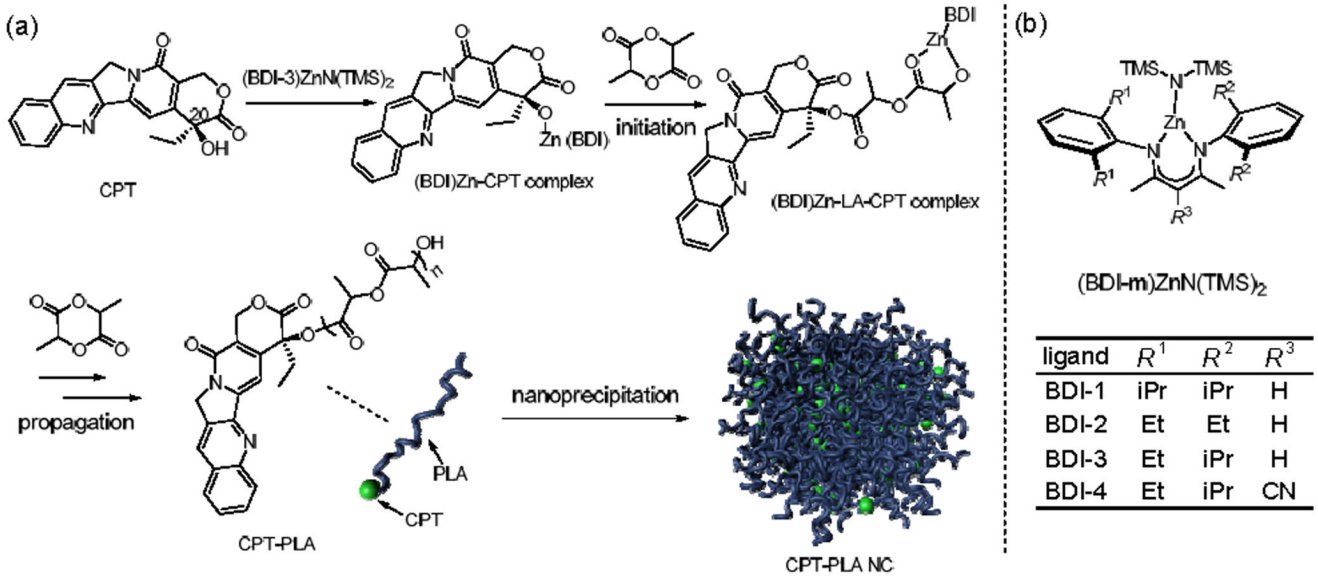

ligand	R^1	R^2	R^3
BDI-1	iPr	iPr	H
BDI-2	Et	Et	H
BDI-3	Et	iPr	H
BDI-4	Et	iPr	CN

Figure 1.

(a) Schematic illustration of (BDI-3)ZnN(TMS)$_2$/CPT mediated ring-opening polymerization of LA to make CPT-PLA conjugates followed by nanoprecipitation of the resulting CPT-PLA conjugates for the preparation of CPT-PLA nanoconjugates; (b) The structure of (BDI-m)ZnN(TMS)$_2$ (m = 1–4).

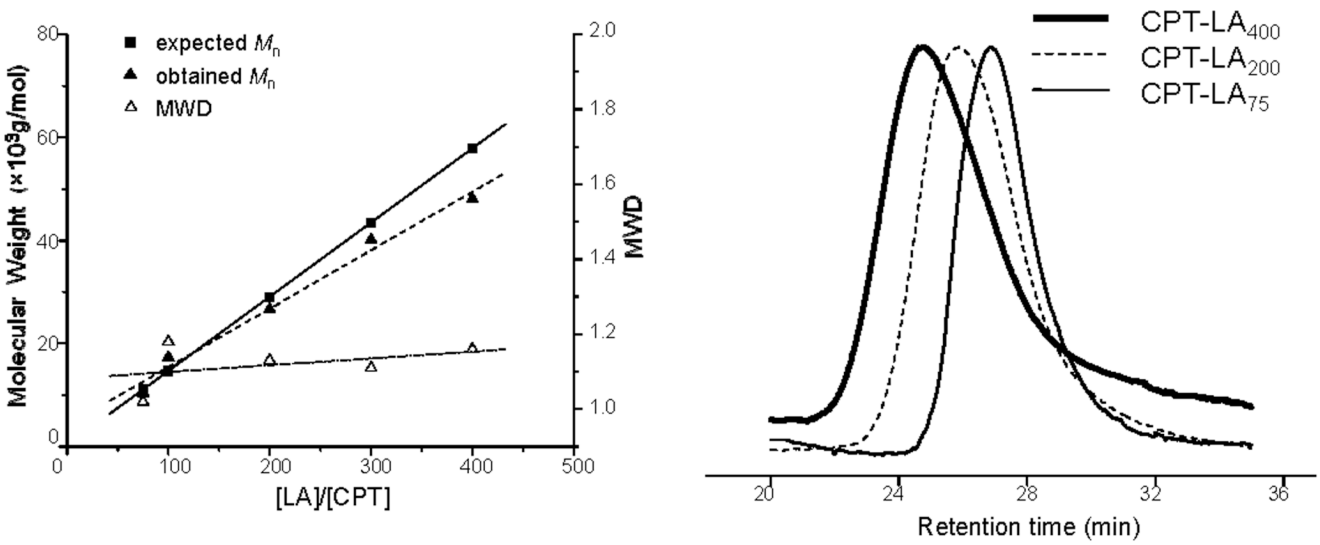

Figure 2.
(a) (BDI-3)ZnN(TMS)$_2$/CPT mediated ring-opening polymerization of LA at various LA/CPT ratios; (b) Overlay of the GPC trace of CPT-LA$_{75}$, CPT-LA$_{200}$ and CPT-LA$_{400}$ prepared by (BDI-3)ZnN(TMS)$_2$/CPT mediated LA polymerizations.

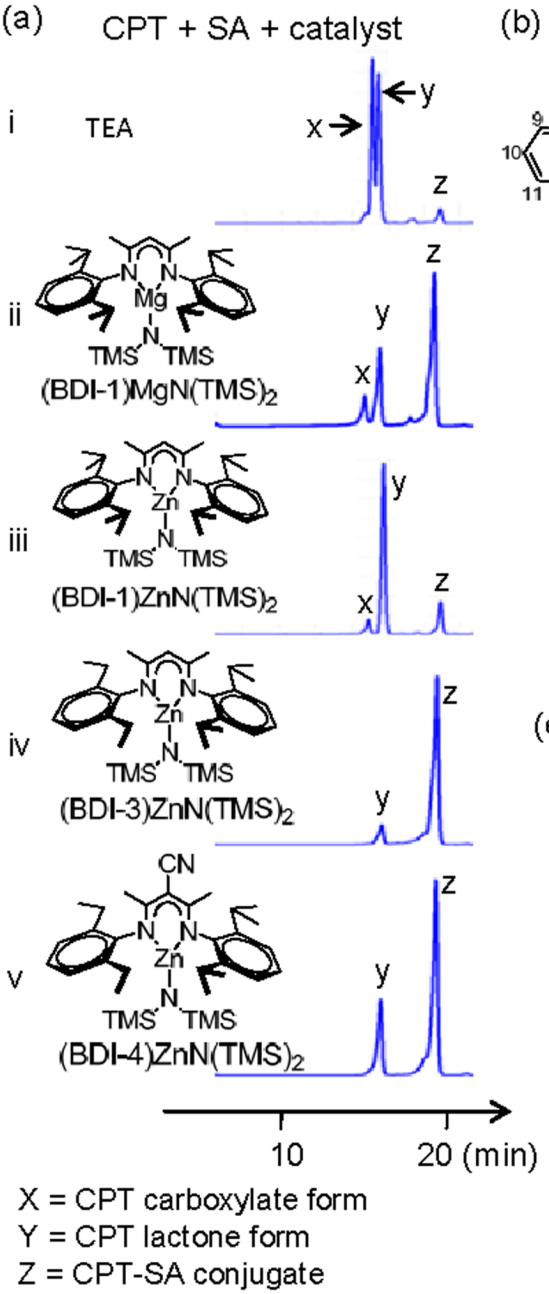

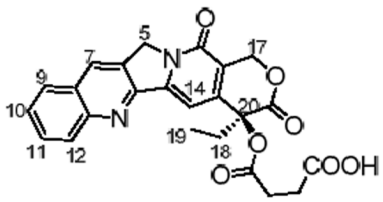

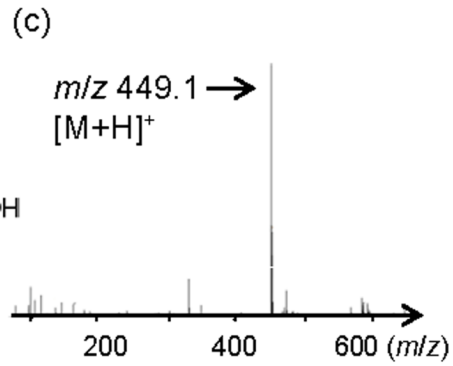

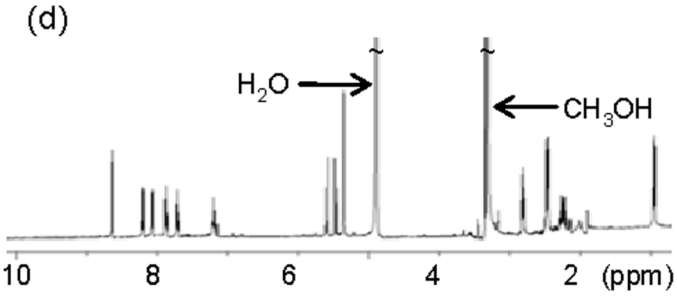

(e)

	CPT-SA (δ, ppm)	CPT (δ, ppm)
7-H	8.63	8.64
12-H	8.21	8.21
9H	8.07	8.07
11-H	7.87	7.87
10-H	7.71	7.72
14-H	7.43	7.46
17-H	5.57, 5.44	5.58, 5.41
5-H	5.35	5.36
-C*H*$_2$-COOH	2.81	
-OC(O)C*H*$_2$-	2.55	
18-H	2.23	1.97
19-H	0.99	1.01

Figure 3.

(a) HPLC analysis of the reaction of SA and CPT in the presence of (i) TEA, (ii) (BDI-1) MgNTMS$_2$, (iii) (BDI-1)ZnNTMS$_2$, (iv) (BDI-3)ZnNTMS$_2$ or (v) (BDI-4)ZnNTMS$_2$; (b) Structure and H-assignment of CPT-SA. (c) ESI-MS of CPT-SA (positive mode). $[M+H]^+$: m/z 449.1. High resolution ESI-MS for $[M+H]^+$ obtained: m/z 449.1355; calculated: m/z 449.1349; (d) ^{1}H NMR of CPT-SA (CD_3OD, 500 MHz). (e) The chemical shift values of CPT and CPT-SA derived from the corresponding ^{1}H-NMR spectra

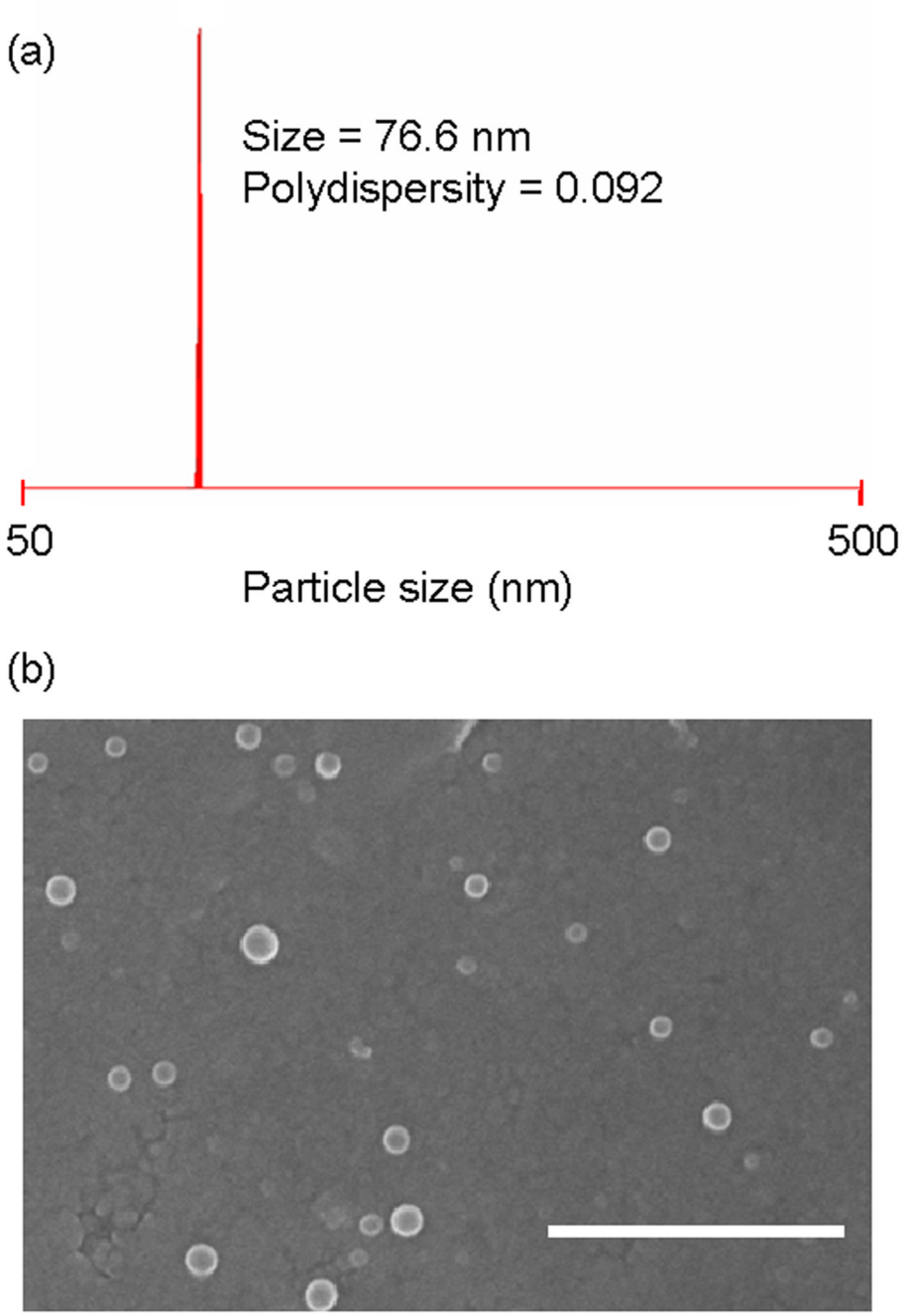

Figure 4.
(a) Analysis of the particle size and size distribution of CPT-LA_{25} NC by DLS. (b) Scanning electron microscope (SEM) image of CPT-LA_{25} NC. Scale bar = 1.0 μm

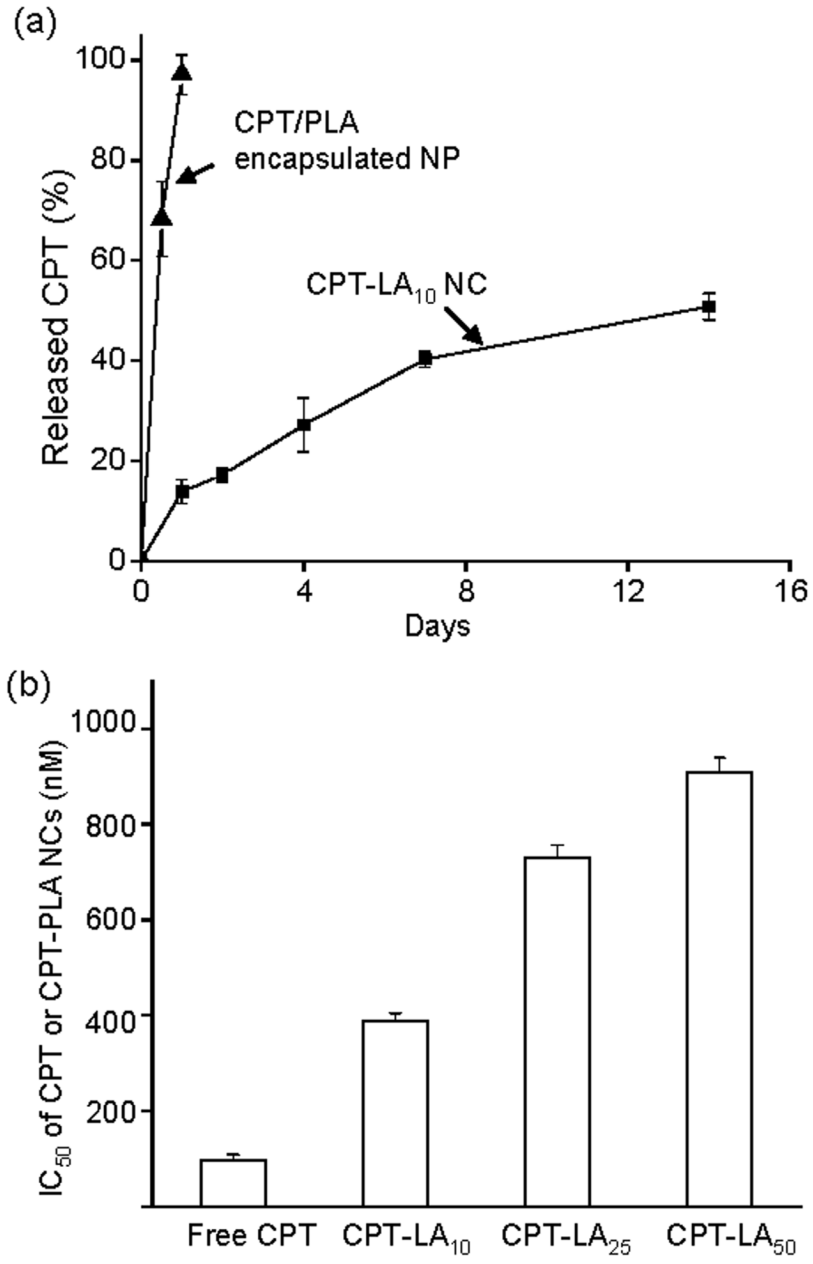

Figure 5.

(a) Release of CPT from the CPT-LA_{10} NC (■) and the CPT/PLA NP prepared by encapsulation (▲, CPT/PLA = 5/95 (wt/wt)); (b) MTT assay to evaluate the cytotoxicity of CPT-LA_{10}, CPT-LA_{25}, CPT-LA_{50} NCs and CPT in PC-3 cell (37°C, 72 h).

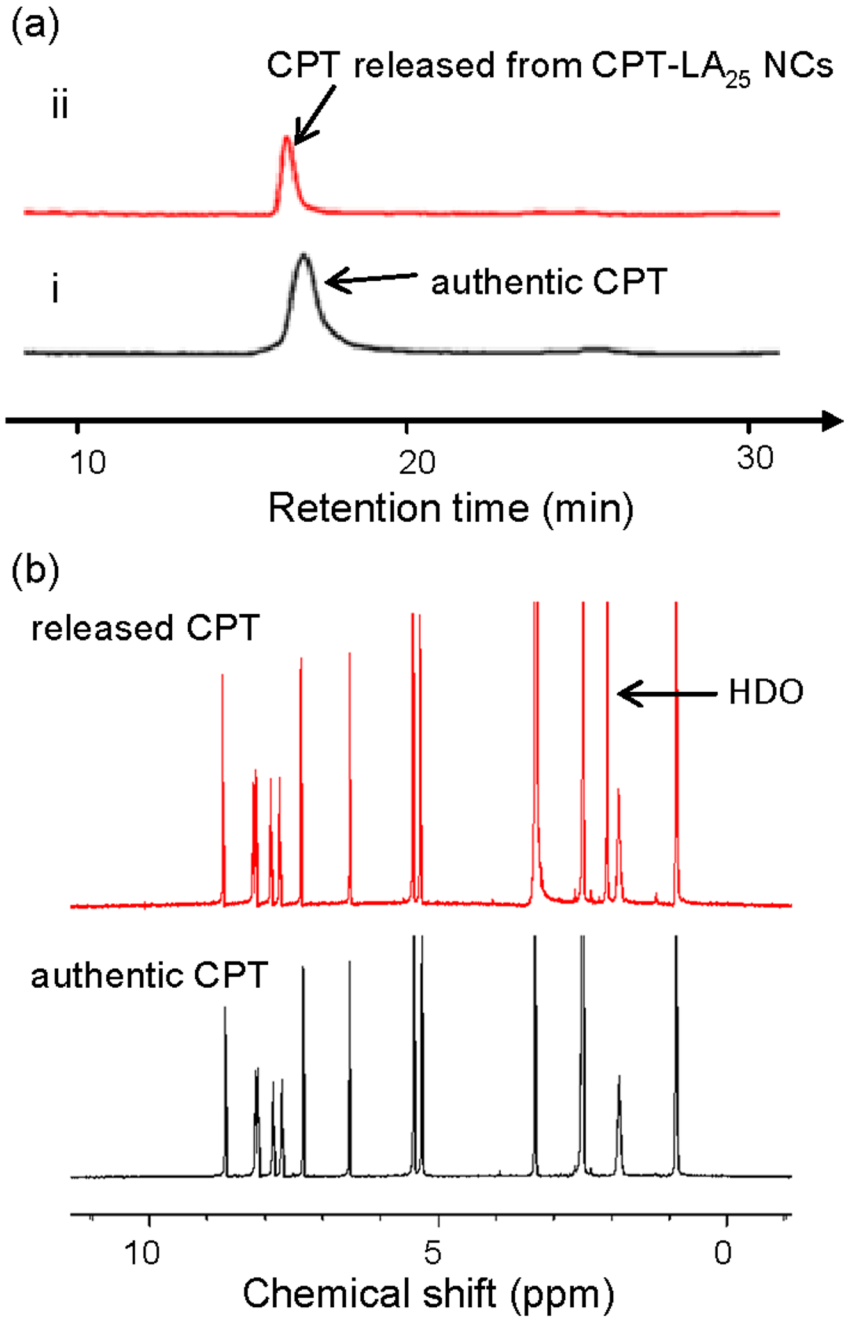

Figure 6.

(a) Overlay of the HPLC spectrum of (a) authentic CPT and (b) CPT released from CPT-LA_{25} NC (incubated in PBS for 2 days at 37°C. (b) ^{1}H NMR spectrum (DMSO-d^{6}) of the CPT released from CPT-LA_{25} and collected on a preparative RP HPLC, and compared with the ^{1}H NMR spectrum of the authentic CPT

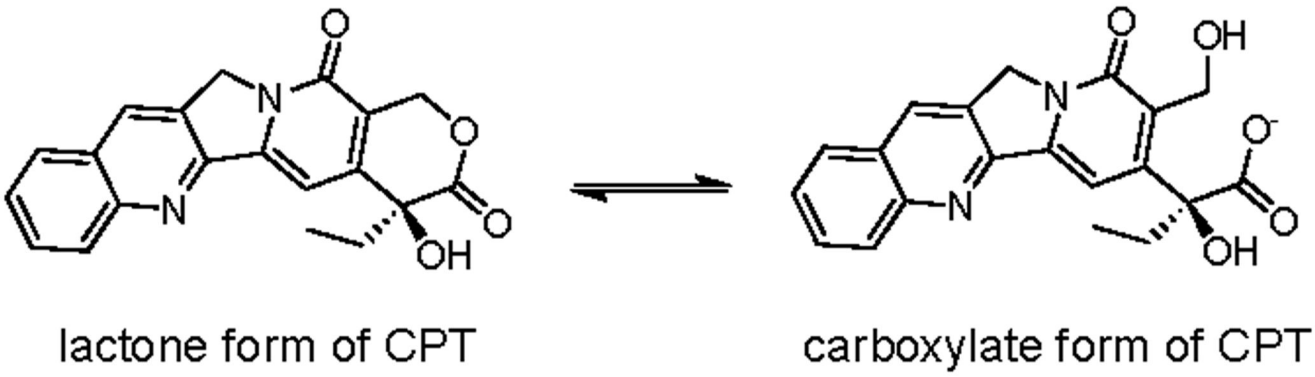

lactone form of CPT carboxylate form of CPT

Scheme 1.
Equilibrium of CPT Lactone and Carboxylate Forms

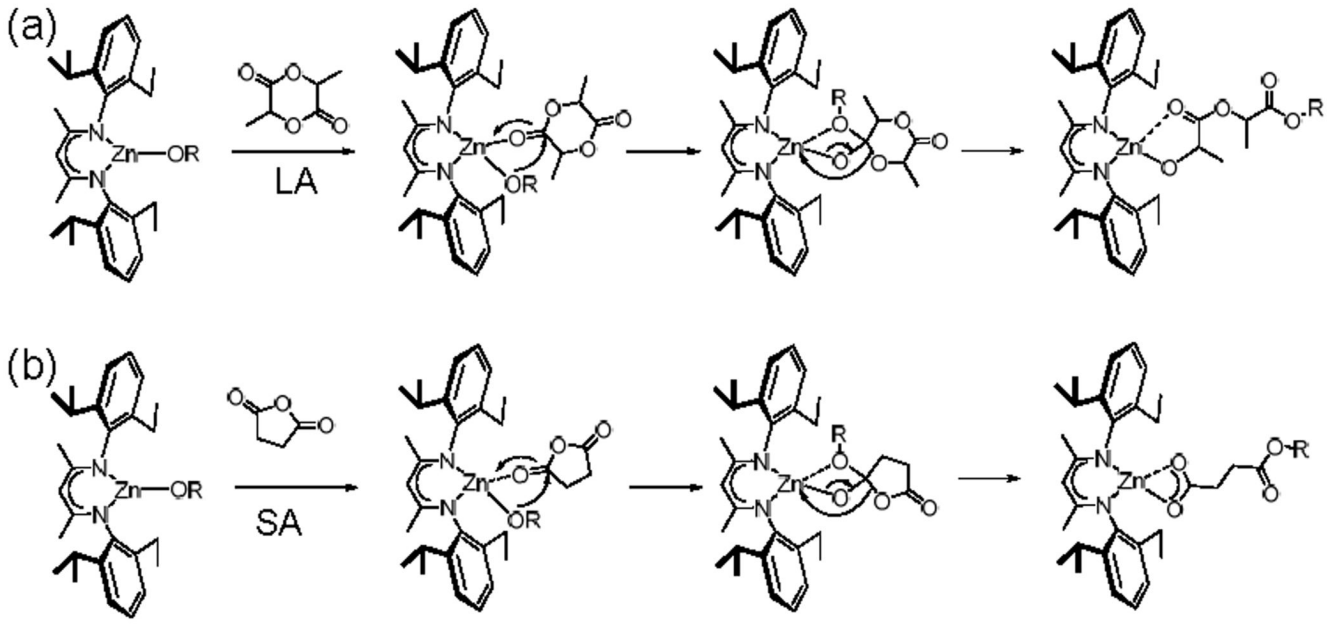

Scheme 2.
Suggested Insertion–Coordination Mechanism of (BDI)Zn-OR Mediated Ring Opening of (a) LA and (b) SA.

Table 1

CPT/(BDI)MN(TMS)$_2$ Mediated LA Polymerization (M = Zn or Mg).[a]

entry	catalyst	temp.	IE (%)[b]	CV (%)[c]	M_n (×10^{4}g/mol)	MWD (M_w/M_n)
1	(BDI-1)MgN(TMS)$_2$	r.t.	>99	>99	1.13	1.31
2	(BDI-1)ZnN(TMS)$_2$	r.t.	61	>99	2.83	1.07
3	(BDI-2)ZnN(TMS)$_2$	r.t.	>99	>99	2.01	1.20
4	(BDI-3)ZnN(TMS)$_2$	r.t.	>99	>99	1.73	1.18
5	(BDI-4)ZnN(TMS)$_2$	r.t.	0	0	ND	N.D
6	(BDI-4)ZnN(TMS)$_2$	40 °C	>98	>98	1.12	1.32

[a] All reactions were performed at a LA/CPT/catalyst ratio of 100:1:1.01 in anhydrous THF for 12 h ([LA]$_0$= 0.69 M). The expected M_n of CPT-PLA conjugate = 1.47 × 10^4 g/mol. Abbreviation: LA = lactide; CPT = camptothecin; temp. = temperature; IE = incorporation efficiency or initiation efficiency, which is the percent of therapeutic agent utilized in the initiation of LA polymerization; the IE is equivalent to the encapsulation efficiency utilized in making nanoparticles via non-covalent, encapsulation strategy; CV = conversion of LA; ND = not determined.

[b] Determined by the HPLC measurement of the unreacted CPT in the polymerization solution.

[c] Determined by monitoring the IR band of the LA lactone at 1772 cm^{-1}.

Table 2

CPT/(BDI-3)ZnN(TMS)$_2$ Mediated LA Polymerization at Various LA/CPT Ratios.[a]

entry	[LA]/[CPT]	IE (%)[b]	CV (%)[c]	$M_{n\ Cal}$ (×10^{3}g/mol)	M_n (×10^{3}g/mol)	MWD (M_w/M_n)
1	75	>99	>99	11.1	10.4	1.02
2	100	>99	>99	14.7	17.3	1.18
3	200	>99	>99	29.1	26.6	1.13
4	300	>99	>99	43.5	40.1	1.11
5	400	>99	>99	57.9	48.0	1.16

[a] All reactions were performed in anhydrous THF for 12 h at room temperature ([LA]$_0$= 0.69 M). Abbreviation: LA = lactide; CPT = camptothecin; IE = incorporation efficiency or initiation efficiency, which is the percent of therapeutic agent utilized in the initiation of LA polymerization; the IE is equivalent to the encapsulation efficiency utilized in making nanoparticles via non-covalent, encapsulation strategy;

[b] Determined by the HPLC measurement of the unreacted CPT in the polymerization solution.

[c] Determined by monitoring IR band of LA lactone at 1772 cm^{-1}.

Table 3

Ring Opening of Succinic Anhydride (SA) by CPT in the Presence of TEA, EDC/DMAP or (BDI)MN(TMS)$_2$ (M = Mg or Zn).[a]

entry	temp. (°C)	catalyst	solvent	time (h)	yield (%)[c]
1	r.t	/	THF	24	0
2	40	TEA	THF	12	10.6
3	40	EDC/DMAP[b]	pyridine	12	12.8
4	40	(BDI-1)MgN(TMS)$_2$	THF	4	59.5
5	40	(BDI-1)ZnN(TMS)$_2$	THF	4	18.8
6	40	(BDI-3)ZnN(TMS)$_2$	THF	4	89.1
7	40	(BDI-4)ZnN(TMS)$_2$	THF	4	71.7

[a] All reactions were performed at a SA/CPT/catalyst ratio of 1.1:1:1 ([SA]$_0$= 0.01 M). Abbreviation: SA = succinic anhydride; CPT = camptothecin; TEA = triethylamine; temp. = temperature; EDC = N-(3-dimethylaminopropyl)-N′-ethylcarbodiimide; DMAP = 4-dimethylaminopyridine;

[b] [EDC]/[DMAP]=4/1.

[c] Determined by the HPLC measurement of the CPT-succinic ester (CPT-SA) generated in the reaction solution.

Table 4

Preparation and Characterization of CPT-PLA NCs.[a]

NC	[LA]/[CPT]	LD (%)	CV (%)	IE (%)	NC sizes ± SD (nm)	PD ± SD
CPT-LA_{100}	100	2.36	>99	>99	80.6 ± 0.8	0.083 ± 0.016
CPT-LA_{50}	50	4.61	>99	>99	70.7 ± 0.7	0.096 ± 0.007
CPT-LA_{25}	25	8.82	>99	>99	76.6 ± 0.9	0.092 ± 0.006
CPT-LA_{10}	10	19.48	>99	>99	72.5 ± 0.7	0.056 ± 0.015

[a]Abbreviations: NC = nanoconjugates; LD = CPT loading in wt%; CV = conversion of LA; IE = incorporation efficiency or initiation efficiency, which is the percent of therapeutic agent utilized in the initiation of LA polymerization; the IE is equivalent to the encapsulation efficiency utilized in making nanoparticles via non-covalent, encapsulation strategy; PD = polydispersity of NCs; STD = standard deviation.